Research Article

Journal of PeptideScience

Received: 18 October 2011 Revised: 17 December 2011 Accepted: 20 December 2011 Published online in Wiley Online Library: 16 March 2012

(wileyonlinelibrary.com) DOI 10.1002/psc.2395

Self-assembly of short peptides composed of only aliphatic amino acids and a combination of aromatic and aliphatic amino acids

Chilukuri Subbalakshmi,[a] Sunkara V. Manorama[b] and Ramakrishnan Nagaraj[a]*

The morphology of structures formed by the self-assembly of short N-terminal *t*-butyloxycarbonyl (Boc) and C-terminal methyl ester (OMe) protected and Boc-deprotected hydrophobic peptide esters was investigated. We have observed that Boc-protected peptide esters composed of either only aliphatic hydrophobic amino acids or aliphatic hydrophobic amino acids in combination with aromatic amino acids, formed highly organized structures, when dried from methanol solutions. Transmission and scanning electron microscopic images of the peptides Boc-Ile-Ile-OMe, Boc-Phe-Phe-Phe-Ile-Ile-OMe and Boc-Trp-Ile-Ile-OMe showed nanotubular structures. Removal of the Boc group resulted in disruption of the ability to form tubular structures though spherical aggregates were formed. Both Boc-Leu-Ile-Ile-OMe and H-Leu-Ile-Ile-OMe formed only spherical nanostructures. Dynamic light scattering studies showed that aggregates of varying dimensions were present in solution suggesting that self-assembly into ordered structures is facilitated by aggregation in solution. Fourier transform infrared spectroscopy and circular dichroism spectroscopy data show that although all four of the protected peptides adopt well-defined tertiary structures, upon removal of the Boc group, only H-Phe-Phe-Phe-Ile-Ile-OMe had the ability to adopt β-structure. Our results indicate that hydrophobic interaction is a very important determinant for self-assembly and presence of charged and aromatic amino acids in a peptide is not necessary for self-assembly. Copyright © 2012 European Peptide Society and John Wiley & Sons, Ltd.

Keywords: beta structure; hydrophobic peptides; self-assembly; nanotubes; spherical nanostructures

Introduction

The ability of peptides to self-assemble to form supramolecular structures has been the subject of intense research in recent years [1–12]. Assembly of peptides into highly ordered one-dimensional and three-dimensional nanostructures has been of great interest in the design of electronic materials [13–15], tissue engineering scaffolds [16–18] and drug release [19,20]. Self-aggregating peptides show considerable variations in length, hydrophobicity and the number of charged residues and exhibit considerable structural polymorphism in the aggregated state [1–12]. Proteins or peptides can self-assemble to form nanotubes [21–29]. Peptides such as benzyloxycarbonyl (Z)-Phe-Phe-OH, *t*-butyloxycarbonyl (Boc)-Phe-Phe-OH [30,31], H-Phe-Phe-Phe-OH [31], fluorenylmethoxycarbonyl (Fmoc)-Phe-Phe-OH [32], Fmoc dipeptides made up of combinations of Gly, Ala, Leu, Phe [33] and Boc-βPhe-βPhe-DPro-Gly-βPhe-βPhe-OMe [34], self-assemble which is facilitated by π–π interactions. Even short peptides such as H-Phe-Phe-OH have the ability to form nanosize quantum dots and nanotubes [29]. Short peptides also have the ability to form hydrogels when dissolved in mixtures of organic solvents and water [35–38]. Although dipeptides or tripeptides would not be expected to fold into well-defined secondary structures as monomers, they form highly organized self-assembled structures on forming hydrogels or microporous organic materials [39,40]. Protected short hydrophobic peptides exhibit poor solubility in water but are highly soluble in organic solvents. In this paper, we show that short fully protected hydrophobic peptides without net positive or negative charge, when dissolved in methanol (MeOH) and dried on surfaces, form nanostructures. Protected peptide esters composed of only aliphatic hydrophobic amino acids form nanotubes or globular structures depending on the amino acid composition. The structures are modulated when aromatic amino acids are introduced.

Materials and Methods

Peptide Synthesis

The following peptides have been used in our present study.

Boc-protected peptides: Boc-Ile-Ile-OMe (Boc-II-OMe), Boc-Leu-Ile-Ile-OMe (Boc-LII-OMe), Boc-Phe-Phe-Phe-Ile-Ile-OMe (Boc-FFFII-OMe) and Boc-Trp-Ile-Ile-OMe (Boc-WII-OMe).

Corresponding Boc-deprotected peptides: H-Ile-Ile-OMe (II-OMe), H-Leu-Ile-Ile-OMe (LII-OMe), H-Phe-Phe-Phe-Ile-Ile-OMe (FFFII-OMe) and H-Trp-Ile-Ile-OMe (WII-OMe). The synthesis of these peptides using solution phase methods was carried out as reported earlier [41].

Purity of peptides was characterized using HPLC on Agilent Technologies 1200 Series instrument using a reversed-phase column (Bio Rad Hi-Pore RP 304, 250 × 4.6 mm), with a linear

* *Correspondence to: R. Nagaraj, CSIR-Centre for Cellular and Molecular Biology, Uppal Road, Hyderabad 500 007, India. E-mail: nraj@ccmb.res.in*

a *CSIR-Centre for Cellular and Molecular Biology, Uppal Road, Hyderabad 500 007, India*

b *CSIR-Indian Institute of Chemical Technology, Nanomaterials Laboratory, Uppal Road, Hyderabad 500 007, India*

gradient of 0.1% TFA in H_2O to 0.1% TFA in acetonitrile : isopropanol (iPrOH) (7 : 3) in 55 min. The molecular masses were confirmed on an electrospray ionization mass spectrometer with a linear ion trap mass analyzer (LTQ-IT, Thermo Fischer, Waltham, MA, USA). The purity of all the HPLC-purified peptides was ≥98%. HPLC-purified peptides were used for all studies.

Sample Preparation

Methanol solutions of both Boc-protected and Boc-deprotected peptide esters (10 mg/ml, w/v) were prepared and centrifuged in an Eppendorf centrifuge at 20879 g for 30 min at room temperature. No residue was observed visually. The 10-mg/ml solutions were diluted to 5 and 2 mg/ml. The peptide solutions were immediately used for morphological characterization.

Transmission Electron Microscopy

The peptide solutions were adsorbed for approximately 30 s at ambient conditions onto formvar/carbon-coated 200-mesh copper grids and then stained with 2% (w/v) uranyl acetate for 30 s before blotting out excess solvent. The MeOH samples dried in 5–10 min. The samples were examined with a JEM-2100 (M/S JEOL Ltd, Tachikawa, Tokyo, Japan) transmission electron microscopy (TEM) at 100 kV accelerating voltage.

Scanning Electron Microscopy

The peptide solutions (20 μl) in MeOH were dried on a cover slip. Dried peptide films were sputter-coated with 50% Au/50% Pd with SC7 620 sputter coater unit (Polaron Range). Images were captured on a Hitachi S-3400N Scanning Electron Microscopy (SEM) (Hitachi Science Systems Ltd, Hitachinaka, Japan) at an accelerated voltage of 10 kV.

Dynamic Light Scattering

The average hydrodynamic radii were measured by recording the scatter at 90°, within a few minutes of dissolving the peptides, using Flexible Correlator Photocor-FC (JDS Uniphase) Dynamic Light Scattering (DLS) instrument (Photocor Instruments, Beltsville MD, USA). The hydrodynamic radii were calculated using the distribution analysis method based on multipass algorithm to process the time-dependent correlation function data (light scattering intensity) using DynaLS software.

Attenuated Total Internal Reflection Fourier Transform Infrared Spectroscopy

Infrared spectra were obtained at a resolution of 4 cm^{-1} on a Fourier transform instrument (Bruker ALPHA-T, Bruker Optik, Ettlingen, Germany) equipped with a single-reflection diamond-attenuated total reflectance accessory. Peptide solutions (20 μl) were dried on the surface of the diamond crystal element by evaporating the solvent. Twenty scans were recorded at 200 cm^{-1} min scan speed and averaged.

Circular Dichroism Spectroscopy

The CD spectra were recorded on Jasco J-815 spectropolarimeter (Jasco, Tokyo, Japan). Peptide solutions (2 mg/ml) were scanned in the far UV range between 190 and 250 nm, and 5-mg/ml solutions were used for recording the near UV range CD spectra between 250 and 300 nm. The spectra were recorded using 8–12 repetitive scans at a rate of 100 nm/min, band width of 1 nm, response time of 0.5 s and a sample interval of 0.2 nm in 1-mm light path demountable cells. The instrument was calibrated with (+)-10-camphorsulfonic acid (1 mg/ml), and the ellipticity was expressed as the mean residue ellipticity, $[\theta]_{MRE}$ (deg cm^2/dmol).

Conductance

The electrical conduction of peptides dried from MeOH stocks was measured using two-terminal transport experiments on interdigitated electrodes using Keithley 236 source I/V measure unit (Keithley Instruments, Inc. Cleveland, OH, USA). The devices for these measurements consisted of interdigitated electrodes with 0.5-mm gaps. Peptides were deposited on the electrodes using cast deposition of a 10-μl drop of 10 mg/ml. Measurements were carried out after solvent evaporation. The voltage was increased linearly from 0.1 to 2 V in 0.1-V steps, and the resultant current was measured. Control experiments on empty devices (i.e. without peptides) and also with Boc-protected amino acids were carried out.

Results and Discussion

Dipeptides with hydrophobic residues have been used to generate microporous organic materials [39]. The crystal structure of Ile-Ile obtained from trifluoroethanol is interesting as the observed pores are comparable with those formed by Phe-Phe and contains co-crystallized solvent molecules in the channels. Also, it was possible to replace the solvent, post-crystallization [39]. Hence, the Ile-Ile-dipeptide sequence was chosen. In order to examine self-association in the absence of electrostatic interactions, the fully protected peptide was used for the investigations. The dipeptide Ile-Ile sequence was elongated using Leu rather than Ile in Boc-LII-OMe to examine the effect of introducing a strong helix-forming amino acid in a sequence that has β-structure propensity. The Phe-Phe-Phe sequence has been shown to have higher network propensities and increased aggregate stability as compared with Phe-Phe [31]. Hence, the sequence was used to generate Boc-FFFII-OMe. In order to examine the effect of varying the aromatic group, Trp was introduced to obtain Boc-WII-OMe. The Boc-protected as well as the N-free peptide esters were used in the study.

The morphology of self-assembled Boc-protected and deprotected peptides in MeOH was studied using TEM, SEM and DLS. The secondary structures of the self-assembled structures were examined using Fourier transform infrared spectroscopy (FT-IR) and CD spectroscopy.

The HPLC elution profiles of both protected and deprotected peptides on reversed-phase C18 column were examined. The retention time and percentage of MeCN/iPrOH (7 : 3) at which the peptides eluted (mentioned in parenthesis) were Boc-II-OMe:] (38.4 min, 69.8%), Boc-LII-OMe: (41.5 min, 75.45%), Boc-FFFII-OMe: (45.6 min, 82.9%) and Boc-WII-OMe: (41.6 min, 75.6%). The retention times varied considerably indicating that the hydrophobicities are different. Based on their retention times, Boc-II-OMe and Boc-FFFII-OMe were the least and the most hydrophobic peptides, respectively. The retention times suggest that Boc-LII-OMe and Boc-WII-OMe have similar hydrophobicities.

Self-Assembly of Peptides Visualized using Electron Microscopy

The TEM image of Boc-II-OMe at 5 mg/ml indicates 5–10-μm-long nanotubes (shown by a thick arrow) with diameter ~250–300 nm

Journal of PeptideScience

(Figure 1A). Figure 1B shows the SEM image of Boc-II-OMe at 10 mg/ml. The image indicates the association of these fibrillar structures that entwine to form bundles of 1–2 μm thickness. Removal of the Boc group from Boc-II-OMe resulted in disruption of nanotubular structures as seen in the TEM image (Figure 1C). Spherical aggregates or spherical nanostructures with diameter of ~50–100 nm (shown by a dotted arrow) are observed that appear to form clusters.

In order to examine the effect of increasing the hydrophobicity and introducing a strong helix-forming amino acid in a sequence that has strong β-structure propensity, on self-assembly, the aggregation behavior of both Boc-LII-OMe and LII-OMe was examined. The TEM and SEM images of Boc-LII-OMe (Figure 2A and B, respectively) show spherical nanostructures. Similarly, the TEM and SEM images of LII-OMe (Figure 2C and D, respectively) show spherical nanostructures. Diameter of the globular structures varied between 100 and 300 nm. Increasing the hydrophobicity appeared to favor formation of spheres rather than rods. The globular structures formed by Boc-LII-OMe are organized and not amorphous. Both leucine and isoleucine residues have propensities for inducing ordered secondary structures in a polypeptide chain [42]. Leucine is considered to be the strongest α-helix–forming residue. Isoleucine, because of bulky methyl group at the β-position, strongly favors β-conformation. The structural propensity of the amino acids also appears to make an important contribution to the morphology of the self-assembled structures.

Self-assembly of phenylalanine-containing peptides in aqueous solutions have been investigated extensively [26,29,31,43–47]. Interactions between aromatic residues play an important role in promoting self-assembly in these peptides. Hence, we examined the aggregation behavior of Boc-FFFII-OMe in which aromatic interactions would be possible in addition to hydrophobic interactions between the aliphatic side chains of isoleucine. TEM images of Boc-FFFII-OMe also show the presence of long, tubular rodlike structures with diameter ~300–500 nm (shown by thick arrows) (Figure 3A and B). SEM image of Boc-FFFII-OMe shows dense rods (shown by a thick arrow) that self-assembled to form membrane-like network (Figure 3C). Removal of the Boc group resulted in disruption of the ability to form tubular structures as seen in the TEM and SEM images that depict mainly globular structures with ~100–500 nm diameters (Figure 3D and E, respectively).

To examine the effect of varying aromatic residue on aggregation, Trp residue was added to obtain Boc-WII-OMe. TEM image shows structural polymorphism. Figure 4A shows both branched tubular structures (shown by a thick arrow) of ~100–200 nm diameter and globular structures of ~500 nm diameter (shown by a dotted arrow) from which tubular structures appear to be growing. In the SEM image, large globular structures of ~200 nm diameter size (shown by a dotted arrow) are observed from which branched tubular structures of about 100–300 nm diameter (shown by a thick arrow) appear to bud out (Figure 4B). On the contrary, only globular structures are seen in the SEM

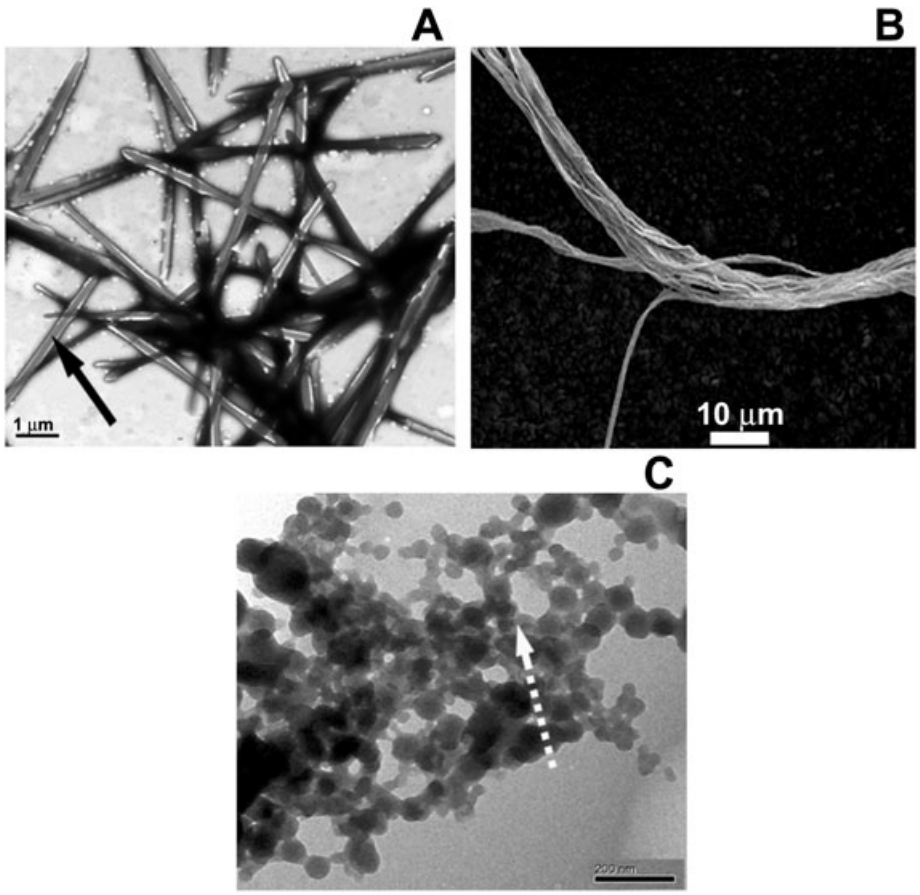

Figure 1. (A) TEM image of 5 mg/ml Boc-II-OMe, (B) SEM image of 10 mg/ml Boc-II-OMe, and (C) TEM image of 10 mg/ml II-OMe.

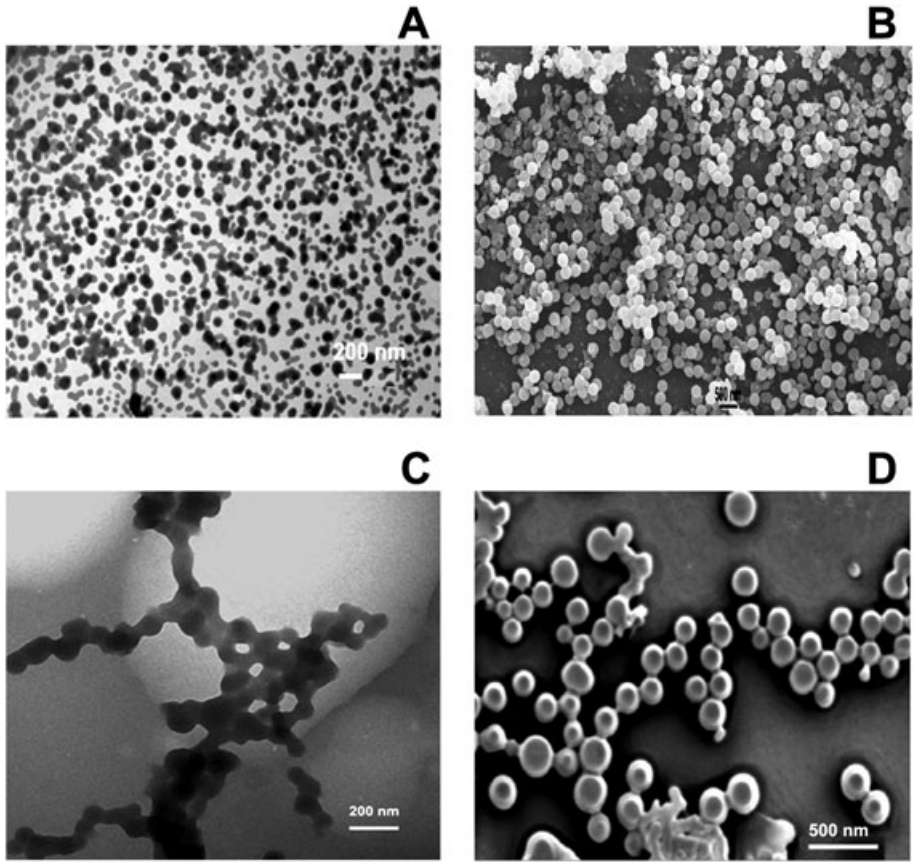

Figure 2. (A) TEM image of 5 mg/ml Boc-LII-OMe, (B) SEM image of 10 mg/ml Boc-LII-OMe, and (C) TEM and (D) SEM images of LII-OMe. Peptide concentration = 10 mg/ml in MeOH for panels C and D.

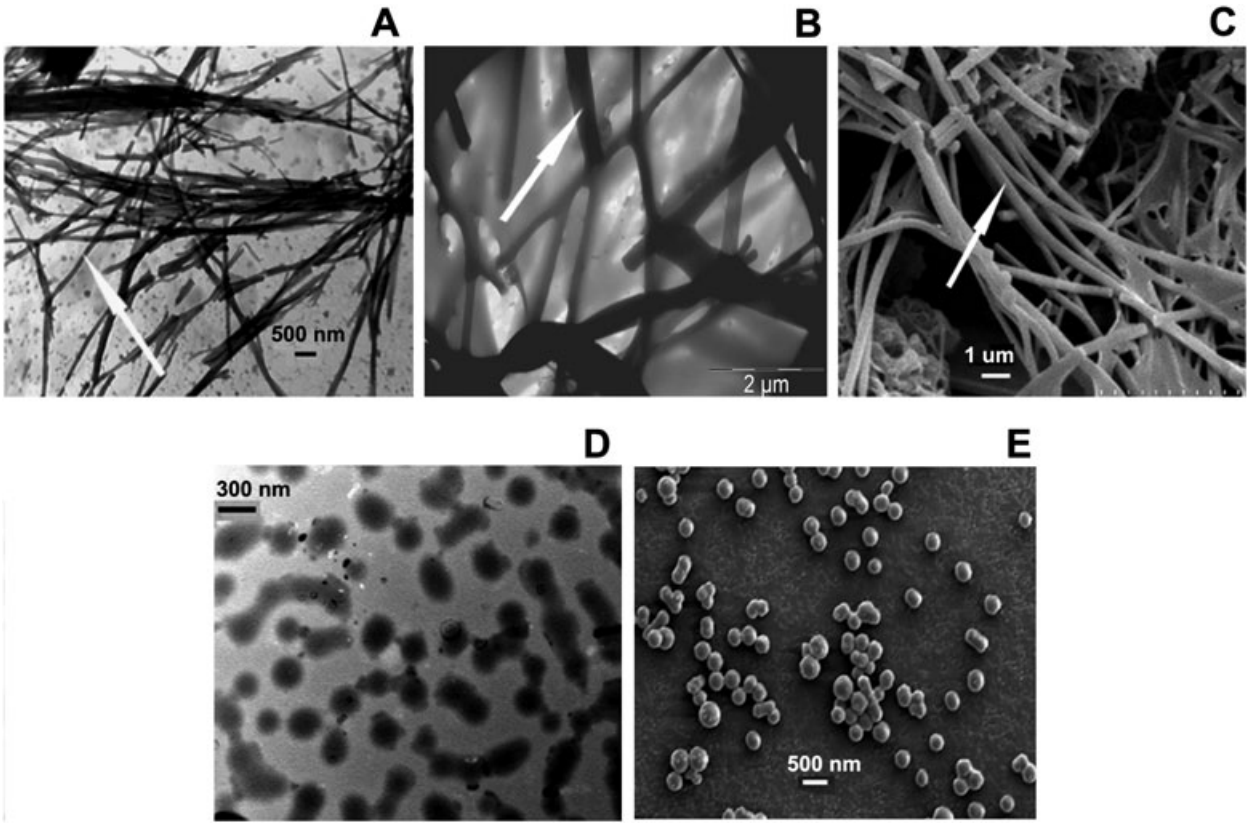

Figure 3. (A and B) TEM and (C) SEM images of Boc-FFFII-OMe. (D) TEM and (E) SEM images of FFFII-OMe. Peptide concentration = 10 mg/ml in MeOH.

Journal of PeptideScience

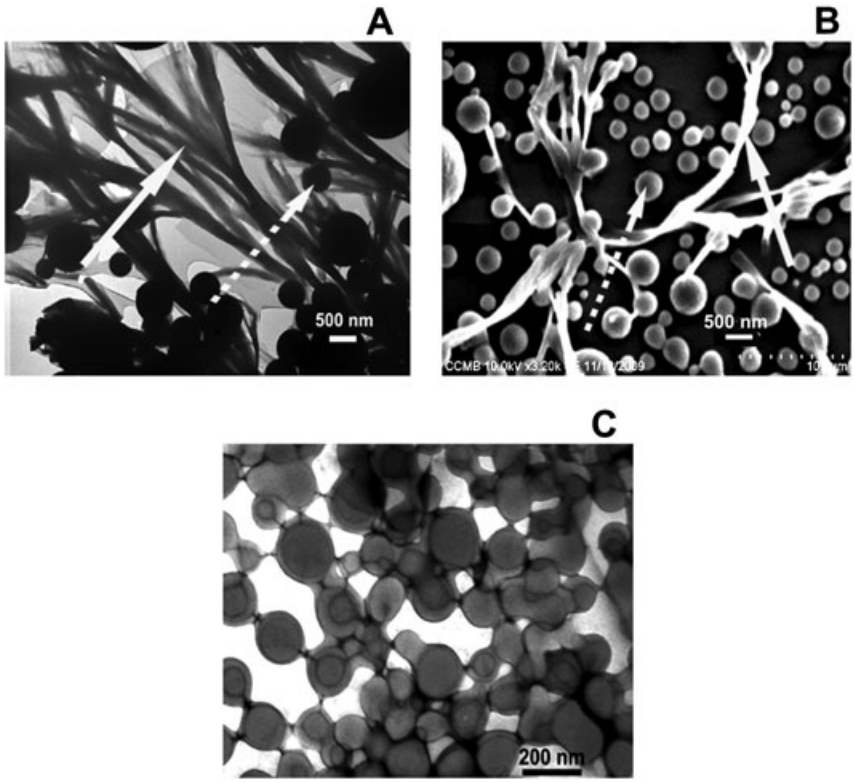

Figure 4. (A) TEM and (B) SEM images of Boc-WII-OMe. (C) SEM image of WII-OMe. Peptide concentration = 10 mg/ml in MeOH.

image of WII-OMe (Figure 4C). It was observed that the deprotected peptides, FFFII-OMe and WII-OMe, with high content of aromatic residues assembled into vesicles and not into tubular structures as observed for the corresponding protected peptides. Presence of a free -NH_2 group appears to favor self-association into globular structures. This could be because the Boc group must also be playing a crucial role in facilitating intermolecular hydrogen bond formation.

Dynamic Light Scattering

In order to determine whether the peptides aggregate in solution, their DLS profiles were examined. DLS profiles of Boc-protected and deprotected peptides suggest the formation of multimodal and polydisperse structures with varying average hydrodynamic radii (R_h) that could be related to their aggregation ability in MeOH solutions (Figure 5). Although the structures observed using TEM and SEM may not be present in solution, rapid drying could result in a supersaturation state that facilitates the formation of numerous nucleation sites on the surface causing the formation of the observed structures as proposed for phenylalanine-containing dipeptides [47].

Attenuated Total Internal Reflection FT-IR Spectroscopy

The FT-IR spectrum of Boc-II-OMe (Figure 6A) shows bands at 1625 and 1682 cm^{-1}, suggesting the presence of antiparallel β-sheet conformation [48–55]. An additional band at 1648 cm^{-1} suggests the presence of unordered structure [48,55]. The spectrum of Boc-FFFII-OMe that also forms nanotubes shows a band at 1636 cm^{-1} (Figure 6C) suggesting β-sheet conformation [48–51]. The varying morphologies of Boc-II-OMe and Boc-FFFII-OMe can be attributed to difference in the arrangement of β-sheets that is reflected in the IR spectra. Boc-LII-OMe and Boc-WII-OMe that do not form tubelike structures show a band at 1642 cm^{-1} (Figure 6E and G). Although the region 1640–1650 cm^{-1} is attributed to the presence of unordered conformation [48,55], we argue that this peak arises because of the peptides in ordered conformation, as distinctive structures that are observed are unlikely to arise if the peptides populate unordered conformation. The spectra of Boc-deprotected peptides are different from those of the protected peptides with the exception of FFFII-OMe (±Boc). Because ordered structures albeit different from the protected peptides are also observed using TEM and SEM, we assign the IR spectra to ordered, rather than unordered, conformation (Figure 6, right-hand panels). II-OMe exhibited a prominent band at 1665 cm^{-1} in the amide I region (Figure 6B). Clearly, the structures formed by II-OMe are not composed of β-structures as in Boc-II-OMe. The spectra of both Boc-FFFII-OMe and FFFII-OMe exhibited a prominent band at 1636 cm^{-1} in the amide I region, indicating β-sheet structure (Figure 6C and D). The IR spectra of both LII-OMe and WII-OMe show a broad band at ~1646 cm^{-1} and a shoulder at 1666 cm^{-1} that were assigned unordered and turn structure, respectively (Figure 6F and H), indicating the presence of mixed population [56,57].

CD Spectroscopy

Because aromatic residues particularly when present in short peptides are likely to contribute substantially to the signal in the far UV region, the CD spectra of only Boc-II-OMe and Boc-LII-OMe and their deprotected variants were examined in the far UV region (Figure 7). The spectrum of Boc-II-OMe shows a broad minimum at ~225 nm and a band with positive ellipticity

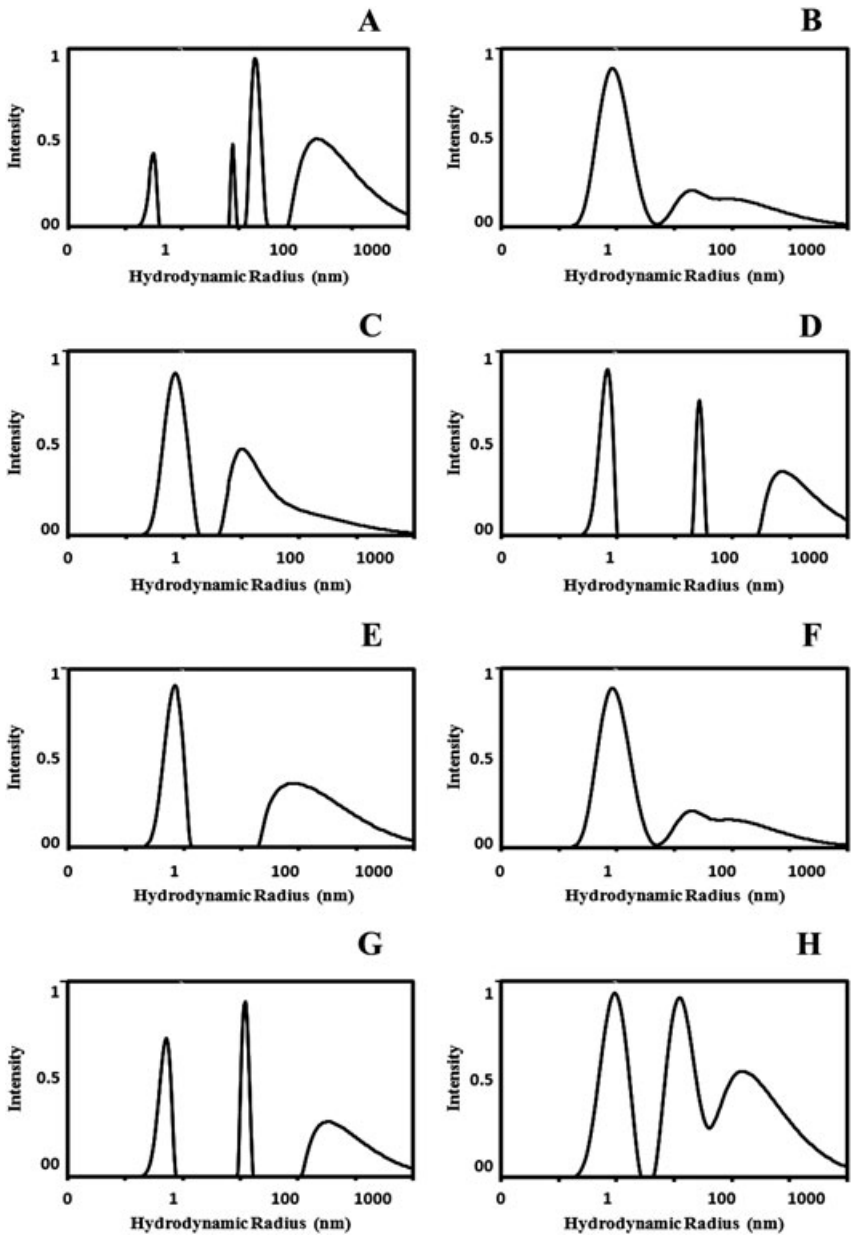

Figure 5. The hydrodynamic radii (R_h) of the Boc-protected and deprotected peptides in MeOH calculated from the DLS data: (A) Boc-II-OMe, (B) II-OMe, (C) Boc-LII-OMe, (D) LII-OMe, (E) Boc-FFFII-OMe, (F) FFFII-OMe, (G) Boc-WII-OMe, and (H) WII-OMe. Peptide concentration = 5 mg/ml.

at 202 nm (Figure 7A). Boc-LII-OMe shows a broad minimum at ~225 nm with a shoulder at 205 nm (Figure 7C). The spectra suggest the presence of β-sheet structures that could arise by self-association of the peptides because the peptides cannot form turns or β-hairpin structures. The β-sheet structures formed by Boc-II-OMe and Boc-LII-OMe are different as indicated by their CD spectra. The differences in the orientation of the strands could give rise to the different morphologies observed for the two peptides using TEM and SEM. On removal of the Boc group, both peptides exhibit a prominent positive band (Figure 7B and D). The spectra are similar to those obtained for peptides derived from $A\beta_{16-22}$ sequence KLVFFAE [58]. The occurrence of prominent positive bands in these peptides have been attributed to self-assembled structures facilitated by stacking interactions between residues. Our results indicate that self-assembly of non-aromatic peptides result also in positive bands in the CD spectra. The observation of prominent bands in the region 250–300 nm (Figure 8) indicates the presence of ordered self-assembled structures in solution for Boc-FFFII-OMe and Boc-WII-OMe. The near UV CD spectra of the peptides with aromatic amino acids in MeOH were recorded. Boc-FFFII-OMe (Figure 8A) exhibited three negative bands at 252, 259 and 265 nm and two negative local maxima at 255 and 262 nm [59,60]. The near UV CD spectra of Boc-WII-OMe (Figure 8B) showed complex broad vibrational fine structure with maxima at ~275, ~282 nm, ~286 and ~290 nm. Deprotection of Boc group showed aromatic CD spectra similar to the corresponding Boc-protected peptides. The spectra suggest that the peptides are folded into well-defined structures even in solution [60–62].

Journal of PeptideScience

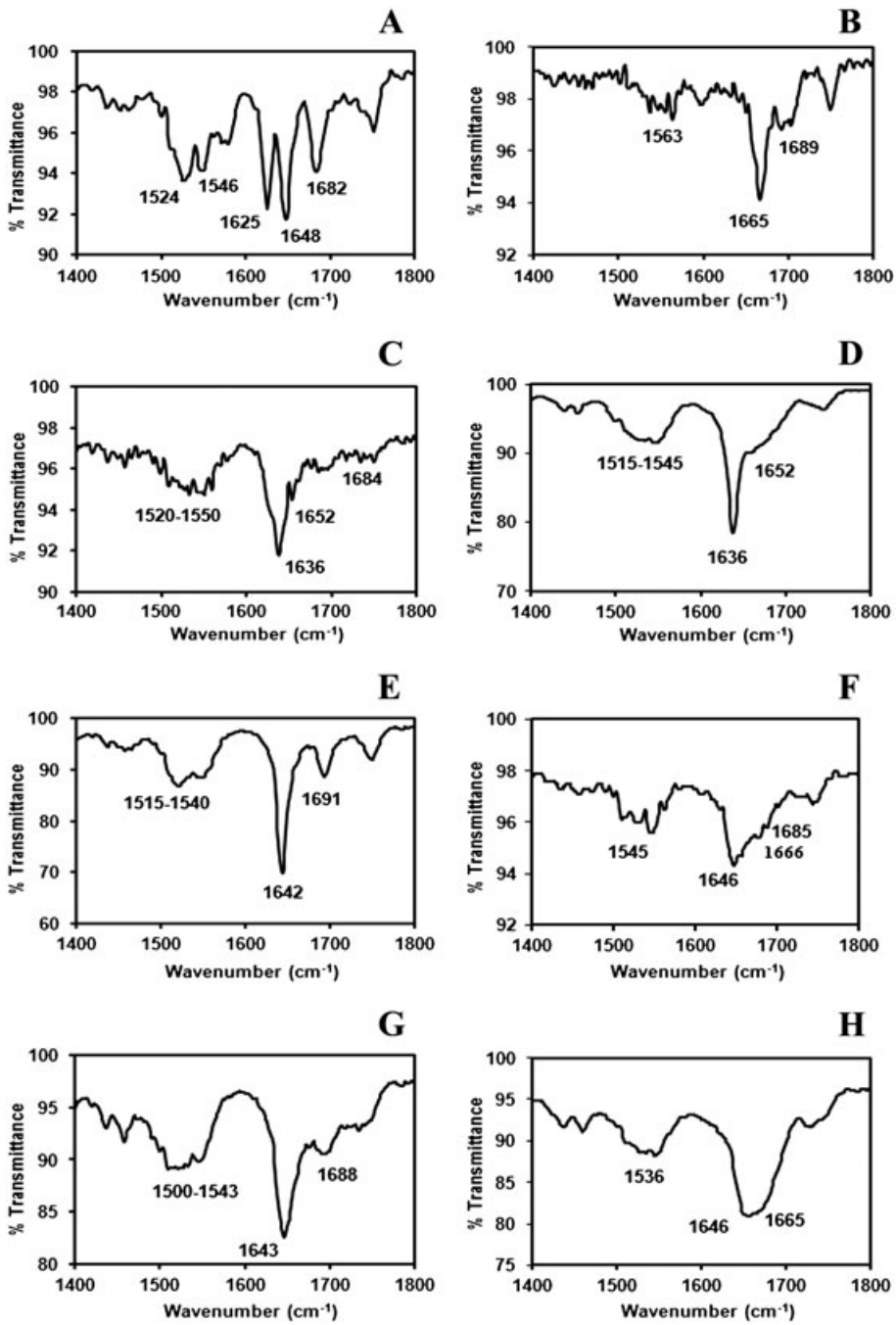

Figure 6. Attenuated total internal reflection FT-IR spectra of dried films of Boc-protected and deprotected peptide esters recorded in the range 1400–1800 cm^{-1}: (A) Boc-II-OMe, (B) II-OMe, (C) Boc-FFFII-OMe, (D) FFFII-OMe, (E) Boc-LII-OMe, (F) LII-OMe, (G) Boc-WII-OMe, and (H) WII-OMe. Peptide concentration = 10 mg/ml in MeOH.

Conductance

Conductance of peptides was examined by depositing peptide solution in MeOH and drying on electrodes using cast deposition [63]. Control experiments, where MeOH was dried and samples were prepared from Boc-protected amino acids such as Boc-Ile, Boc-Leu, Boc-Phe and Boc-Trp, revealed very low current signals. The conductance experiments carried out with 10 mg/ml Boc-protected peptide solutions in MeOH are shown in Figure 9. The relative electrical conductance of Boc-protected peptides is greater as compared with their Boc-deprotected counterparts (Figure 9A–D). The change in current as a function of voltage is considerably more for Boc-II-OMe as compared with the other peptides. Although Boc-FFFII-OMe also shows tubelike structures, the conductance is relatively less as compared with Boc-II-OMe that could be because the tubes formed by Boc-FFFII-OMe (<500 nm diameter, 4–10 μm long) are much shorter and thinner than those formed by Boc-II-OMe (>1–2 μm diameter, >10–20 μm long) as seen using SEM. The conductance profiles of LII-OMe and WII-OMe, as compared with II-OMe and FFF-OMe, can be attributed to very low current signals.

The observed increase of electrical conduction is most likely a result of the movement of charges facilitated by hydration shells as proposed for fibrils formed by an elastin-related polypeptide

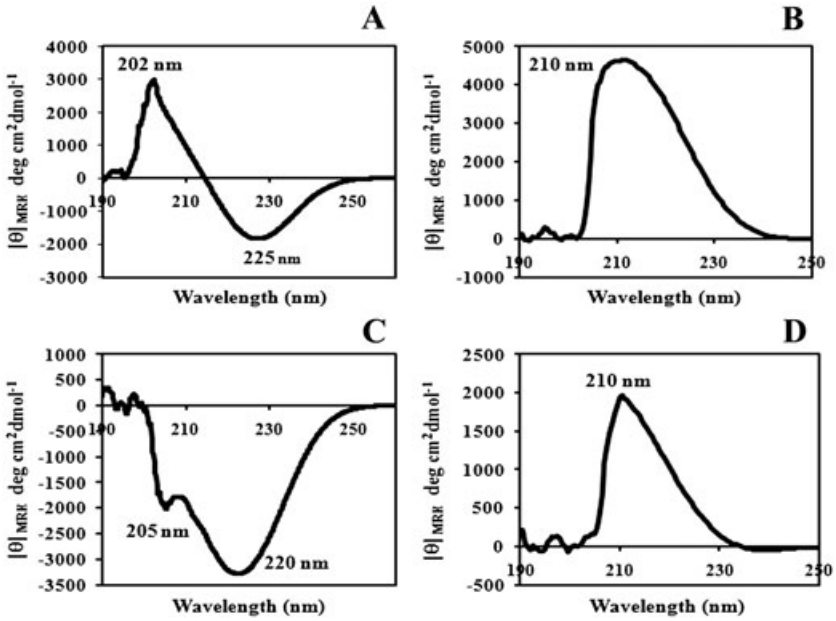

Figure 7. Far UV CD spectra of the both Boc-protected and Boc-deprotected peptides recorded in MeOH between 190 and 250 nm. (A) Boc-II-OMe, (B) II-OMe, (C) Boc-LII-OMe, and (D) LII-OMe. Peptide concentration = 2 mg/ml in MeOH.

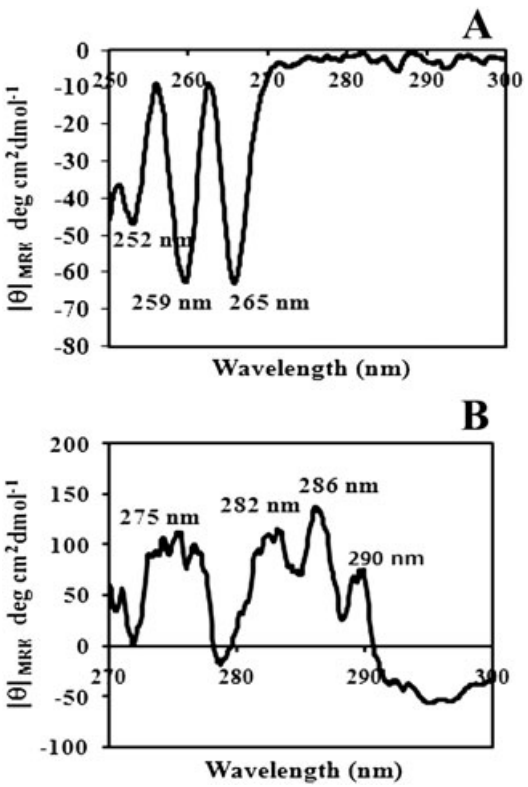

Figure 8. Near UV CD spectra of the Boc-protected peptides recorded in MeOH between 250 and 300 nm. (A) Boc-FFFII-OMe and (B) Boc-WII-OMe. Peptide concentration = 5 mg/ml in MeOH.

[63]. The differences in the conduction indicate that it is a property of the oligomers and does not depend only on the primary sequence of the peptides that form the oligomers. The conductance appears to depend on the nanostructures formed by the peptides because considerable difference in electrical conductance was observed between the peptides Boc-II-OMe and Boc-FFFII-OMe and Boc-WII-OMe. The nanofibrils formed from Boc-II-OMe appear to sustain significant electrical conduction in the solid state at ambient conditions and have remarkable stability.

Conclusions

We have characterized the self-assembly of four different Boc-protected peptide esters and the respective Boc-deprotected peptide esters into various structures. We have shown that short, fully protected peptides, with N-terminal Boc and C-terminal methyl ester protecting groups, tend to self-associate in MeOH at high concentrations, to form organized structures as seen in the TEM/SEM images of dried films. Variations such as presence or absence of the Boc-protecting group show marked differences in the morphological features of the peptides ranging from nanotubular structures to globular aggregates upon drying on surfaces. The far UV CD spectra of Boc-protected aliphatic peptides strongly suggest the presence of β-structures that could form only by self-association, in solution. The near UV CD of both protected and deprotected peptides with aromatic amino acids exhibited peaks indicating well-defined structures. Our results clearly indicate that hydrophobic interaction alone can drive peptides to self-assemble into highly ordered structures. Presence of charged amino acids and aromatic amino acids is not necessary for self-assembly. By judicious positioning of strong helix or β-structure–forming amino acids, it should be possible to generate structures with varying morphologies. Our results offer insights into design of self-assembling peptides that could have potential for various applications.

Acknowledgements

We thank Dr Shashi Singh for assistance in recording electron microscopy images and Ch VB Swamy for mass spectral analysis. Funding for the CSIR network project NWP0035 is gratefully acknowledged. R. N. is the recipient of JC Bose Fellowship from the Department of Science and Technology, India.

Journal of PeptideScience

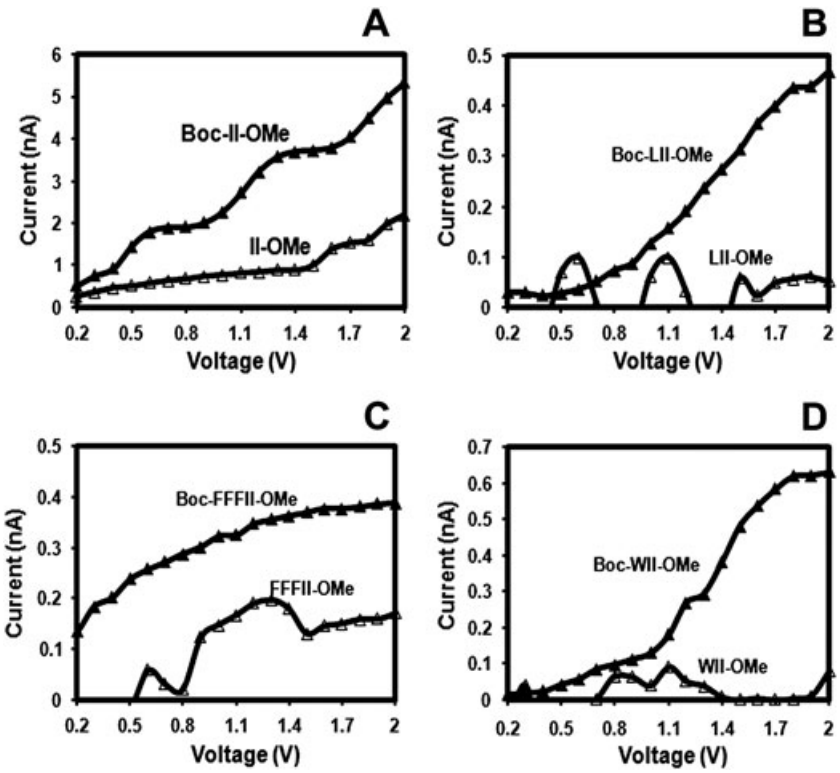

Figure 9. The electrical conduction of peptide nanostructures was measured using two-terminal transport experiments. The voltage was increased linearly from 0.1 to 2 V in 0.1-V steps, and the resultant current was measured. Control experiments on empty devices, MeOH and also with Boc-protected amino acids were carried out and subtracted from the peptide spectra. Peptide concentration = 10 mg/ml in MeOH.

References

1 Aggeli A, Nyrkova IA, Bell M, Harding R, Carrick L, McLeish TCB, Semenov AN, Boden N. Hierarchical self-assembly of chiral rod-like molecules as a model for peptide β-sheet tapes, ribbons, fibrils, and fibers. *Proc. Natl. Acad. Sci. U. S. A.* 2001; **98**: 11857–11862.

2 Chaudhary N, Singh S, Nagaraj R. Organic solvent mediated self-association of an amyloid forming peptide from beta2-microglobulin: an atomic force microscopy study. *Biopolymers* 2008; **90**: 783–791.

3 Chaudhary N, Singh S, Nagaraj R. Morphology of self-assembled structures formed by short peptides from the amyloidogenic protein tau depends on the solvent in which the peptides are dissolved. *J. Pept. Sci.* 2009; **15**: 675–684.

4 Hamley IW. Peptide fibrillization. *Angew. Chem. Int. Ed.* 2007; **46**: 8128–8147.

5 Kreplak L, Aebi U. From the polymorphism of amyloid fibrils to their assembly mechanism and cytotoxicity. *Adv. Protein Chem.* 2006; **73**: 217–233.

6 Lu K, Jacob J, Thiyagarajan P, Conticello VP, Lynn DG. Exploiting amyloid fibril lamination for nanotube self-assembly. *J. Am. Chem. Soc.* 2003; **125**: 6391–6393.

7 Measey TJ, Schweitzer-Stenner R. Aggregation of the amphipathic peptides (AAKA)n into antiparallel β-sheets. *J. Am. Chem. Soc.* 2006; **128**: 13324–13325.

8 Moore RA, Hayes SF, Fischer ER, Priola SA. Amyloid formation via supramolecular peptide assemblies. *Biochemistry* 2007; **46**: 7079–7087.

9 Nuraje N, Su K, Samson J, Haboosheh A, Maccuspie RI, Matsui H. Self-assembly of Au nanoparticle-containing peptide nano-rings on surfaces. *Supramol. Chem.* 2006; **18**: 429–434.

10 Pedersen JS, Otzen DE. Amyloid-a state in many guises: survival of the fittest fibril fold. *Protein Sci.* 2008; **17**: 2–10.

11 Vaden TD, Gowers SAN, de Boer TSJA, Steill JD, Oomens J, Snoek LC. Conformational preferences of an amyloidogenic peptide: IR spectroscopy of Ac-VQIVYK-NHMe. *J. Am. Chem. Soc.* 2008; **130**: 14640–14650.

12 Andersen CB, Hicks MR, Vetri V, Vandahl B, Rahbek-Nielsen H, Thogersen H, Thogersen IB, Enghild JJ, Serpell LC, Rischel C, Otzen DE. Glucagon fibril polymorphism reflects differences in protofilament backbone structure. *J. Mol. Biol.* 2010; **397**: 932–946.

13 Hamedi M, Herland A, Karlsson RH, Inganas O. Electrochemical devices made from conducting nanowire networks self-assembled from amyloid fibrils and alkoxysulfonate PEDOT. *Nano Lett.* 2008; **8**: 1736–1740.

14 Sokolov Y, Kozak JA, Kayed R, Chanturiya A, Glabe C, Hall JE. Soluble amyloid oligomers increase bilayer conductance by altering dielectric structure. *J. Gen. Physiol.* 2006; **128**: 637–647.

15 Xu H, Das AK, Horie M, Shaik MS, Smith AM, Luo Y, Lu X, Collins R, Liem SY, Song A, Popelier PLA, Turner ML, Xiao P, Kinloch IA, Ulijn RV. An investigation of the conductivity of peptide nanotube networks prepared by enzyme-triggered self-assembly. *Nanoscale* 2010; **2**: 960–966.

16 Hartgerink JD, Beniash E, Stupp SI. Self-assembly and mineralization of peptide-amphiphile nanofibers. *Science* 2001; **294**: 1684–1688.

17 Kyle S, Aggeli A, Ingham E, McPherson MJ. Production of self-assembling biomaterials for tissue engineering. *Trends Biotechnol.* 2009; **27**: 423–433.

18 Mart RJ, Osborne RD, Stevens MM, Ulijn RV. Peptide-based stimuli-responsive biomaterials. *Soft Matter* 2006; **2**: 822–835.

19 Gazit E. Molecular self-assembly bioactive nanostructures branch out. *Nat. Nanotechnol.* 2008; **3**: 8–9.

20 Sutton S, Campbell NL, Cooper AI, Kirkland M, Frith WJ, Adams DJ. Controlled release from modified amino acid hydrogels governed by molecular size or network dynamics. *Langmuir* 2009; **25**: 10285–10291.

21 Furuya T, Kiyota T, Lee S, Inoue T, Sugihara G, Logvinova A, Goldsmith P, Ellerby HM. Nanotubules formed by highly hydrophobic amphiphilic [alpha]-helical peptides and natural phospholipids. *Biophys. J.* 2003; **84**: 1950–1959.

22 Ghadiri MR, Granja JR, Milligan RA, McRee DE, Khazanovich N. Self-assembling organic nanotubes based on a cyclic peptide architecture. *Nature* 1993; **366**: 324–327.

23 Görbitz CH. Nanotube formation by hydrophobic dipeptides. *Chem. Eur. J.* 2001; **7**: 5153–5159.

24 Görbitz CH. Nanotubes of L-isoleucyl-L-leucine 0.91-hydrate. *Acta Crystallogr., Sect. E: Struct. Rep.* 2004; **60**: o626–o628.

25 Perutz MF, Finch JT, Berriman J, Lesk A. Amyloid fibers are water-filled nanotubes. *Proc. Natl. Acad. Sci. U. S. A.* 2002; **99**: 5591–5595.
26 Reches M, Gazit E. Formation of closed-cage nanostructures by self-assembly of aromatic dipeptides. *Nano Lett.* 2004; **4**: 581–585.
27 Scanlon S, Amalia A. Self-assembling peptide nanotubes. *Nano Today* 2008; **3**: 22–30.
28 Vauthey S, Santoso S, Gong H, Watson N, Zhang S. Molecular self-assembly of surfactant-like peptides to form nanotubes and nanovesicles. *Proc. Natl. Acad. Sci. U. S. A.* 2002; **99**: 5355–5360.
29 Amdursky N, Molotskii M, Gazit E, Rosenman G. Elementary building blocks of self-assembled peptide nanotubes. *J. Am. Chem. Soc.* 2010; **132**: 15632–15636.
30 Reches M, Gazit E. Casting metal nanowires within discrete self-assembled peptide nanotubes. *Science* 2003; **300**: 625–627.
31 Tamamis P, Adler-Abramovich L, Reches M, Marshall K, Sikorski P, Serpell L, Gazit E, Archontis G. Self-assembly of phenylalanine oligopeptides: insights from experiments and simulations. *Biophys. J.* 2009; **96**: 5020–5029.
32 Mahler A, Reches M, Rechter M, Cohen S, Gazit E. Rigid, self-assembled hydrogel composed of a modified aromatic dipeptide. *Adv. Mater.* 2006; **18**: 1365–1370.
33 Jayawarna V, Ali M, Jowitt TA, Miller AF, Saiani A, Gough JE, Ulijn RV. Nanostructured hydrogels for three-dimensional cell culture through self-assembly of fluorenylmethoxycarbonyl-dipeptides. *Adv. Mater.* 2006; **18**: 611–614.
34 Karle I, Gopi HN, Balaram P. Infinite pleated β-sheet formed by the β-hairpin Boc-β-Phe-β-Phe-D-Pro-Gly-β-Phe-β-Phe-OMe. *Proc. Natl. Acad. Sci. U. S. A.* 2002; **99**: 5160–5164.
35 Adams DJ, Butler MF, Frith WJ, Mark K, Leanne M, Paul S. A new method for maintaining homogeneity during liquid–hydrogel transitions using low molecular weight hydrogelators. *Soft Matter* 2009; **5**: 1856–1862.
36 Debnath S, Shome A, Das D, Das PK. Hydrogelation through self-assembly of Fmoc-peptide functionalized cationic amphiphiles: potent antibacterial agent. *J. Phys. Chem. B* 2010; **114**: 4407–4415.
37 Krysmann MJ, Castelletto V, Kelarakis A, Hamley IW, Hule RA, Pochan DJ. Self-assembly and hydrogelation of an amyloid peptide fragment. *Biochemistry* 2008; **47**: 4597–4605.
38 Orbach R, Adler-Abramovich L, Zigerson S, Mironi-Harpaz I, Seliktar D, Gazit E. Self-assembled Fmoc-peptides as a platform for the formation of nanostructures and hydrogels. *Biomacromolecules* 2009; **10**: 2646–2651.
39 Görbitz C. Microporous organic materials from hydrophobic dipeptides. *Chem. Eur. J.* 2007; **13**: 1022–1031.
40 Cheng G, Castelletto V, Moulton CM, Newby GE, Hamley IW. Hydrogelation and self-assembly of Fmoc-tripeptides: unexpected influence of sequence on self-assembled fibril structure, and hydrogel modulus and anisotropy. *Langmuir* 2010; **26**: 4990–4998.
41 Joseph M, Nagaraj R. Circular dichroism studies on a synthetic peptide corresponding to the membrane-spanning region of vesicular stomatitis virus G protein and its fatty acyl derivative. *Biochim. Biophys. Acta* 1987; **911** 231–237.
42 Chou PY, Fasman GD. Conformational parameters for amino acids in helical, β-sheet, and random coil regions calculated from proteins. *Biochemistry* 1974; **13**: 211–222.
43 Castelletto V, Hamley IW, Harris PJF, Olsson U, Spencer N. Influence of the solvent on the self-assembly of a modified amyloid beta peptide fragment. I. Morphological investigation. *J. Phys. Chem. B* 2009; **113**: 9978–9987.
44 de Groot NS, Parella T, Aviles FX, Vendrell J, Ventura S. Ile-Phe dipeptide self-assembly: clues to amyloid formation. *Biophys. J.* 2007; **92**: 1732–1741.
45 Krysmann MJ, Castelletto V, Hamley IW. Fibrillisation in organic solvent of a hydrophobically modified amyloid peptide fragment. *Soft Matter* 2007; **3**: 1401–1406.
46 Krysmann MJ, Castelletto V, McKendrick JE, Clifton LA, Hamley IW, Harris PJF, King SM. Self-assembly of peptide nanotubes in an organic solvent. *Langmuir* 2008; **24**: 8158–8162.
47 Reches M, Gazit E. Controlled patterning of aligned self-assembled peptide nanotubes. *Nat. Nanotechnol.* 2006; **1**: 195–200.
48 Fink AL, Calciano LJ, Goto Y, Nishimura M, Swedberg SA. Characterization of the stable, acid-induced, molten globule-like state of staphylococcal nuclease. *Protein Sci.* 1993; **2**: 1155–1160.
49 Jaikaran ETAS, Higham CE, Serpell LC, Zurdo J, Gross M, Clark A, Fraser PE. Identification of a novel human islet amyloid polypeptide [beta]-sheet domain and factors influencing fibrillogenesis. *J. Mol. Biol.* 2001; **308**: 515–525.
50 Surewicz WK, Mantsch HH, Chapman D. Determination of protein secondary structure by Fourier transform infrared spectroscopy: a critical assessment. *Biochemistry* 1993; **32**: 389–394.
51 Zandomeneghi G, Mark RHK, Margaret GM, Marcus F. FTIR reveals structural differences between native beta-sheet proteins and amyloid fibrils. *Protein Sci.* 2004; **13**: 3314–3321.
52 Castelletto V, Hamley IW, Harris PJF. Self-assembly in aqueous solution of a modified amyloid beta peptide fragment. *Biophys. Chem.* 2008; **138**: 29–35.
53 Haris PI, Chapman D. The conformational analysis of peptides using Fourier transform IR spectroscopy. *Biopolymers* 1995; **37**: 251–263.
54 Iconomidou VA, Chryssikos GD, Gionis V, Vriend G, Hoenger A, Hamodrakas SJ. Amyloid-like fibrils from an 18-residue peptide analogue of a part of the central domain of the B-family of silkmoth chorion proteins. *FEBS Lett.* 2001; **499**: 268–273.
55 Pelton JT, McLean LR. Spectroscopic methods for analysis of protein secondary structure. *Anal. Biochem.* 2000; **277**: 167–176.
56 Bandekar J, Krimm S. Vibrational analysis of peptides, polypeptides, and proteins: characteristic amide bands of beta-turns. *Proc. Natl. Acad. Sci. U. S. A.* 1979; **76**: 774–777.
57 Krimm S, Bandekar J. Vibrational spectroscopy and conformation of peptides, polypeptides, and proteins. *Adv. Protein Chem.* 1986; **38**: 181–364.
58 Chaudhary N, Nagaraj R. Impact on the replacement of Phe by Trp in a short fragment of Aβ amyloid peptide on the formation of fibrils. *J. Pept. Sci.* 2011; **17**: 115–123.
59 Sreerama N, Manning MC, Powers ME, Zhang J-X, Goldenberg DP, Woody RW. Tyrosine, phenylalanine, and disulfide contributions to the circular dichroism of proteins: circular dichroism spectra of wild-type and mutant bovine pancreatic trypsin inhibitor. *Biochemistry* 1999; **38**: 10814–10822.
60 Woody RW. Circular dichroism. *Methods Enzymol.* 1995; **246**: 34–71.
61 Barth A, Martin SR, Bayley PM. Resolution of Trp near UV CD spectra of calmodulin-domain peptide complexes into the 1La and 1Lb component spectra. *Biopolymers* 1998; **45**: 493–501.
62 Kuwajima K. The molten globule state as a clue for understanding the folding and cooperativity of globular-protein structure. *Proteins: Struct. Funct. Bioinf.* 1989; **6**: 87–103.
63 del Mercato LL, Pompa PP, Maruccio G, Torre AD, Sabella S, Tamburro AM, Cingolani R, Rinaldi R. Charge transport and intrinsic fluorescence in amyloid-like fibrils. *Proc. Natl. Acad. Sci. U. S. A.* 2007; **104**: 18019–18024.

